

On the Multiwavelength Emission of the Intracluster Medium.

Lukasz Stawarz^{1, 2} & Vahe Petrosian³

¹ISAS/JAXA, Japan

²Jagiellonian University, Poland

³KIPAC, Stanford University, USA

ABSTRACT:

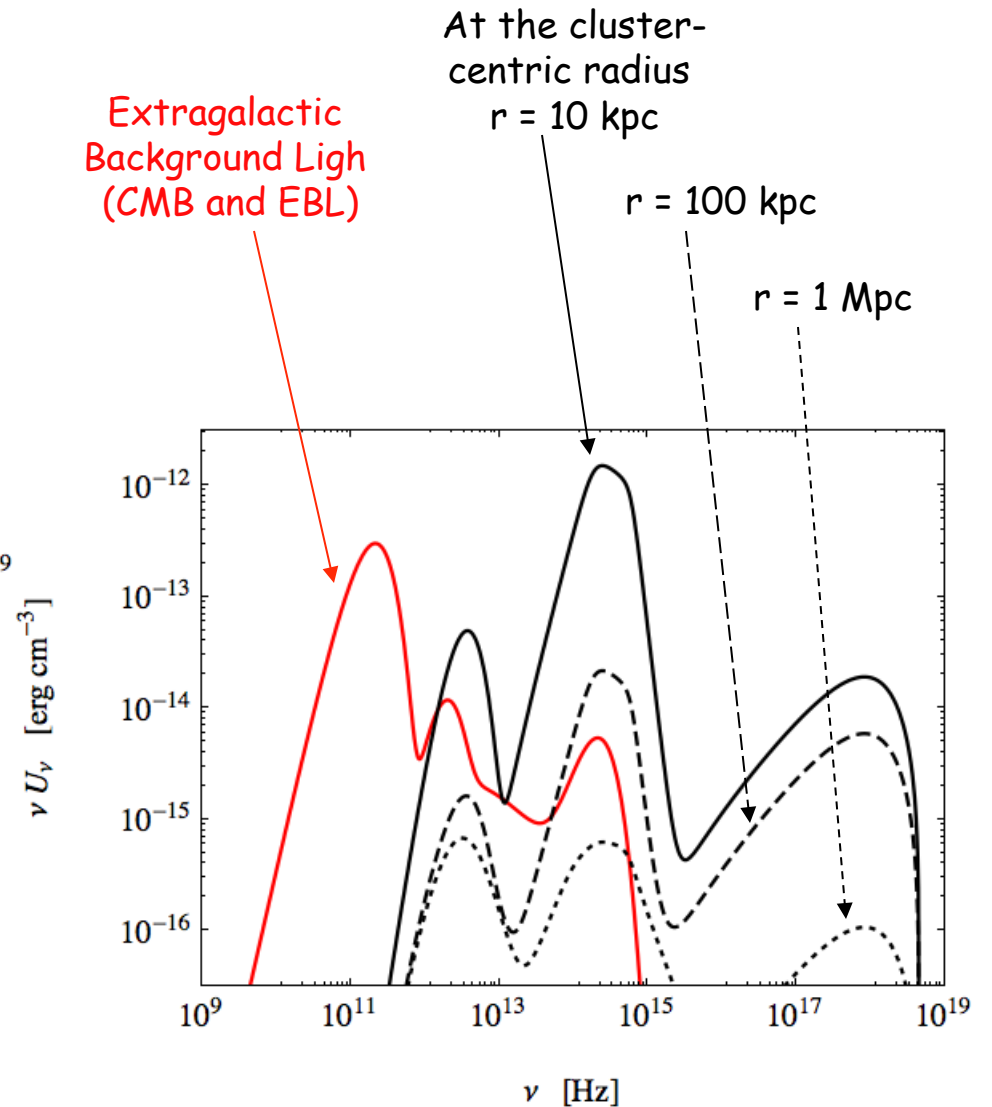
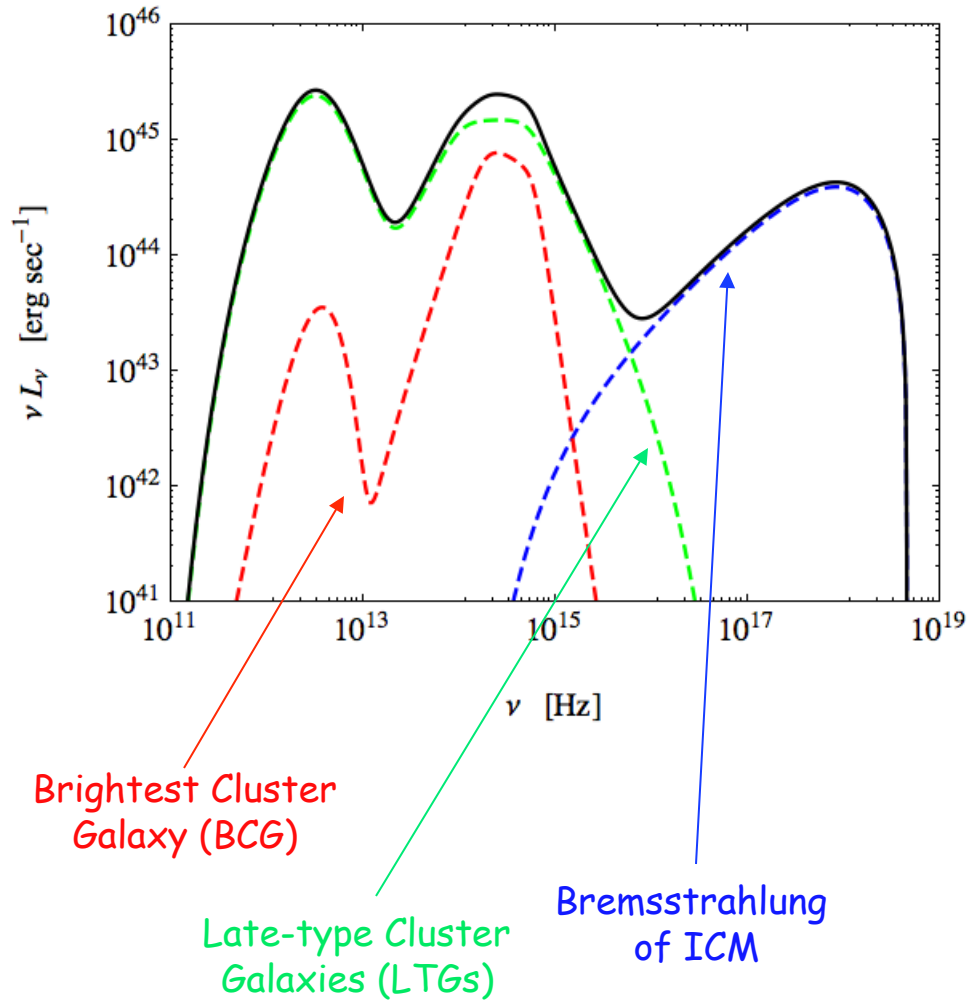
Here we analyze the inverse-Compton (IC) emission of ultrarelativistic electrons present within the intracluster medium (ICM), taking into account not only the Cosmic Microwave Background (CMB) radiation as the seed photon population for the IC scatterings, but also other lower-energy photon fields such as Extragalactic Background Light (EBL) in the infrared-to-optical range, starlight and dust emission of the Brightest Cluster Galaxy (BCG) as well as of all the cluster late-type galaxies (LTGs), or finally the soft X-ray bremsstrahlung radiation of the cluster gas. We show that all these additional populations of the target photons may play an important role in shaping the high-energy emission of clusters, which can in principle be probed in hard X-rays and in gamma-rays by present and planned instruments such as Swift/BAT, ASTRO-H, Fermi/LAT, or modern and future IACTs.

All the considered photon fields differ in spectral properties and in the spatial distribution within a cluster. The total radiative output of a system (including starlight, dust emission, and bremsstrahlung of the ICM) may vary substantially between different sources, depending on the cluster type and particular parameters. Here we assume "typical" values characterizing a rich, post-merger and low-redshift system:

Table 1: Main model parameters.

Parameter	Symbol	Assumed value
central number density of the gas	n_0	0.03 cm^{-3}
gas temperature	T_X	10^8 K
critical radius in the gas distribution	r_{cr}	100 kpc
virial radius of a cluster	r_{vir}	1 Mpc
slope of the gas density distribution	β	0.6
dust temperature in a BCG	T_d	40 K
critical stellar radius in a BCG	r_s	10 kpc
total dust luminosity of a BCG	$L_{d, \text{BCG}}$	$10^{10} L_{\odot}$
total starlight luminosity of a BCG	$L_{s, \text{BCG}}$	$3 \times 10^{11} L_{\odot}$
total X-ray (bremsstrahlung) luminosity of a cluster	L_X	$3 \times 10^{11} L_{\odot}$
total dust luminosity of cluster late-type galaxies	$L_{d, \text{LTGs}}$	$10^{12} L_{\odot}$
total starlight luminosity of cluster late-type galaxies	$L_{s, \text{LTGs}}$	$10^{12} L_{\odot}$
total volume of a cluster	V_{tot}	10^{74} cm^3
volume-averaged gas number density	$\langle n_{\text{icm}} \rangle$	10^{-3} cm^{-3}
total mass of the gas	M_{icm}	$10^{14} M_{\odot}$
total thermal energy of the gas	E_{th}	$3 \times 10^{63} \text{ erg}$
volume-averaged thermal energy density of the gas	$\langle U_{\text{th}} \rangle$	$2 \times 10^{-11} \text{ erg cm}^{-3}$
total energy of the cluster photon fields	$E_{\text{th, rad}}$	$5 \times 10^{59} \text{ erg}$
averaged energy density of the cluster photon fields	$\langle U_{\text{th, rad}} \rangle$	$4 \times 10^{-15} \text{ erg cm}^{-3}$

Total luminosity and energy densities of the starlight, dust emission, and ICM bremsstrahlung for the assumed model parameters.



We anticipate β -profile for the number density of the cluster gas $n_{\text{icm}}(r)$. We also assume that the energy density of the cluster magnetic field $U_B(r) = B^2(r)/8\pi$ follows the gas distribution, so that the Alfvén velocity v_A in the ICM is independent on the distance from the cluster center.

$$n_{\text{icm}}(r) = n_0 \times \left[1 + \left(\frac{r}{r_{\text{cr}}} \right)^2 \right]^{-3\beta/2} \quad B(r) = B_0 \times \left[1 + \left(\frac{r}{r_{\text{cr}}} \right)^2 \right]^{-3\beta/4}$$

For simplicity here we take the ratio of the energy density stored in ultrarelativistic electrons $U_e(r) = \int d\gamma m_e c^2 \gamma n_e(\gamma)$ and in the magnetic field independent on the cluster-centric radius, $\eta_{\text{eq}} = U_e/U_B = \text{const}$. We emphasize that the presented model calculations correspond to **a very small total energy ratios $E_e/E_{\text{th}} < 1\%$**

$$n_e(\gamma > \gamma_{\text{min}}) \propto \gamma^{-s_e} \times \exp \left[-\frac{\gamma}{\gamma_{\text{max}}} \right]$$

For the electron energy distribution we assume a general power-law form. We also consider two different cases (see Petrosian 2001, 2003 for the discussion):

- (1) a relatively young electron population with high-energy cut-off $\gamma_{\text{max}} \gg 10^3$, low-energy cut-off $\gamma_{\text{min}} > 1$, and energy index $s_e = 3$, as appropriate for post-merger clusters hosting giant radio halos,
- (2) an evolved electron population with maximum energies $\gamma_{\text{max}} < 10^3$, minimum energies $\gamma_{\text{min}} \sim 1$, and energy index $s_e = 0$ (resulting from the dominant Coulomb energy losses for cooled electrons), as expected for "relic radio halos".

Table 2: Model A: young radio halo

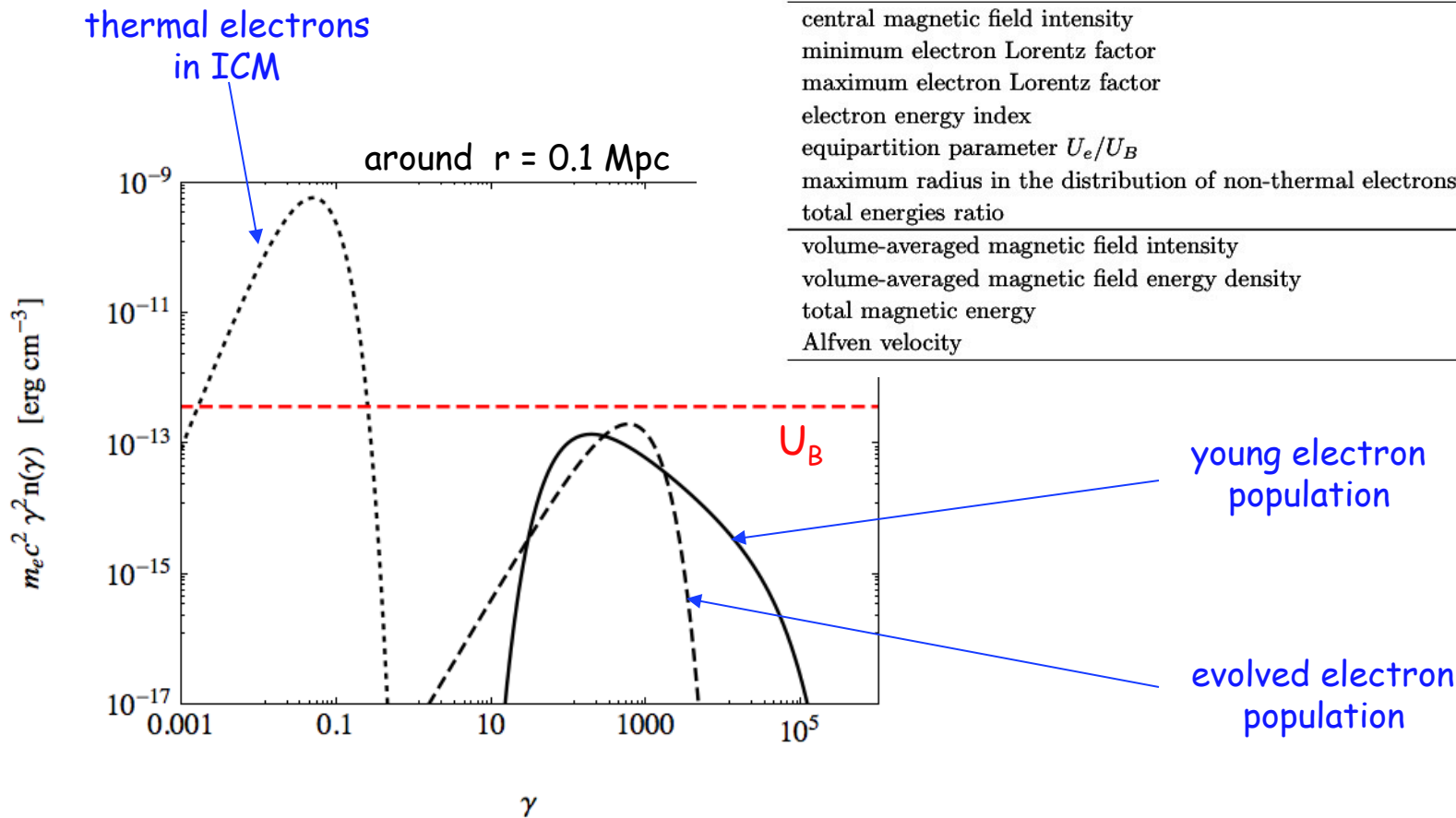
Quantity	Symbol	Model value
central magnetic field intensity	B_0	$3 \mu\text{G}$
minimum electron Lorentz factor	γ_{min}	200
maximum electron Lorentz factor	γ_{max}	3×10^4
electron energy index	s_e	3
equipartition parameter U_e/U_B	η_{eq}	1
maximum radius in the distribution of non-thermal electrons	$r_{\text{max},e}$	r_{vir}
total energies ratio	E_e/E_{th}	5×10^{-4}
volume-averaged magnetic field intensity	$\langle B \rangle$	$0.5 \mu\text{G}$
volume-averaged magnetic field energy density	$\langle U_B \rangle$	$10^{-14} \text{ erg cm}^{-3}$
total magnetic energy	E_B	$2 \times 10^{60} \text{ erg}$
Alfven velocity	v_A	$10^{-4} c$

MODEL A:

- High magnetization
- Electrons distributed within the whole cluster

Table 3: Model A: old radio halo

Quantity	Symbol	Model value
central magnetic field intensity	B_0	$3 \mu\text{G}$
minimum electron Lorentz factor	γ_{min}	1
maximum electron Lorentz factor	γ_{max}	300
electron energy index	s_e	0
equipartition parameter U_e/U_B	η_{eq}	1
maximum radius in the distribution of non-thermal electrons	$r_{\text{max},e}$	r_{vir}
total energies ratio	E_e/E_{th}	5×10^{-4}
volume-averaged magnetic field intensity	$\langle B \rangle$	$0.5 \mu\text{G}$
volume-averaged magnetic field energy density	$\langle U_B \rangle$	$10^{-14} \text{ erg cm}^{-3}$
total magnetic energy	E_B	$2 \times 10^{60} \text{ erg}$
Alfven velocity	v_A	$10^{-4} c$



MODEL A:

- High magnetization
- Electrons distributed within the whole cluster

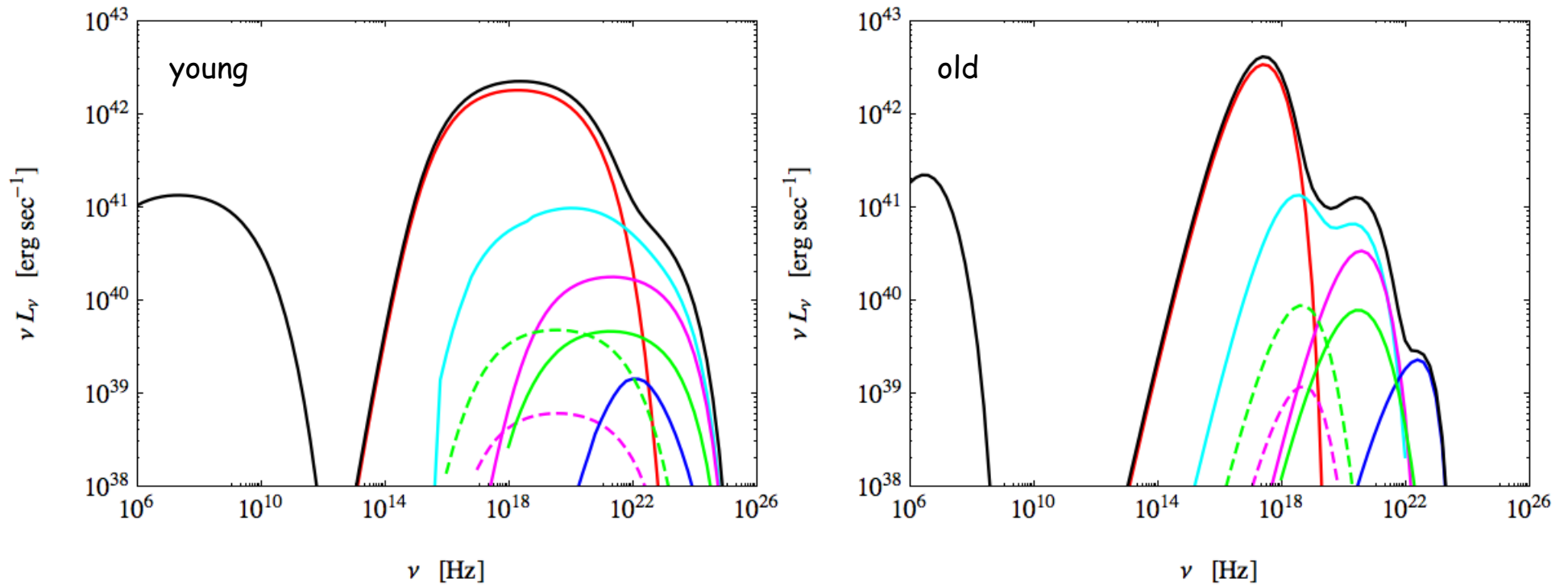


Table 4: Model B: young radio halo

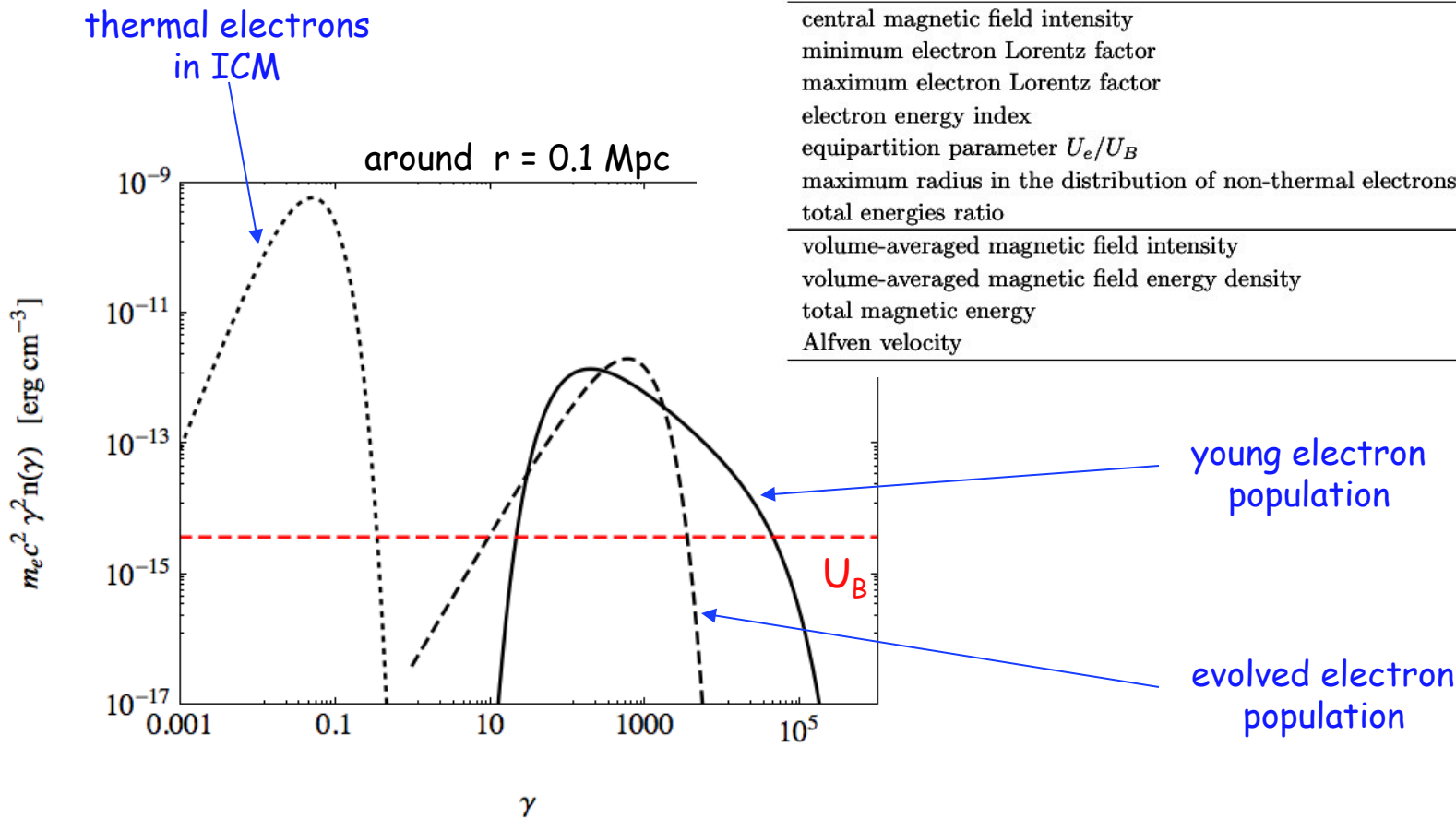
Quantity	Symbol	Model value
central magnetic field intensity	B_0	$0.3 \mu\text{G}$
minimum electron Lorentz factor	γ_{min}	200
maximum electron Lorentz factor	γ_{max}	3×10^4
electron energy index	s_e	3
equipartition parameter U_e/U_B	η_{eq}	10^3
maximum radius in the distribution of non-thermal electrons	$r_{\text{max},e}$	r_{vir}
total energies ratio	E_e/E_{th}	5×10^{-3}
volume-averaged magnetic field intensity	$\langle B \rangle$	$0.05 \mu\text{G}$
volume-averaged magnetic field energy density	$\langle U_B \rangle$	$10^{-16} \text{ erg cm}^{-3}$
total magnetic energy	E_B	$2 \times 10^{58} \text{ erg}$
Alfven velocity	v_A	$10^{-5} c$

MODEL B:

- Low magnetization
- Electrons distributed within the whole cluster

Table 5: Model B: old radio halo

Quantity	Symbol	Model value
central magnetic field intensity	B_0	$0.3 \mu\text{G}$
minimum electron Lorentz factor	γ_{min}	1
maximum electron Lorentz factor	γ_{max}	300
electron energy index	s_e	0
equipartition parameter U_e/U_B	η_{eq}	10^3
maximum radius in the distribution of non-thermal electrons	$r_{\text{max},e}$	r_{vir}
total energies ratio	E_e/E_{th}	5×10^{-3}
volume-averaged magnetic field intensity	$\langle B \rangle$	$0.05 \mu\text{G}$
volume-averaged magnetic field energy density	$\langle U_B \rangle$	$10^{-16} \text{ erg cm}^{-3}$
total magnetic energy	E_B	$2 \times 10^{58} \text{ erg}$
Alfven velocity	v_A	$10^{-5} c$



MODEL B:

- Low magnetization
- Electrons distributed within the whole cluster

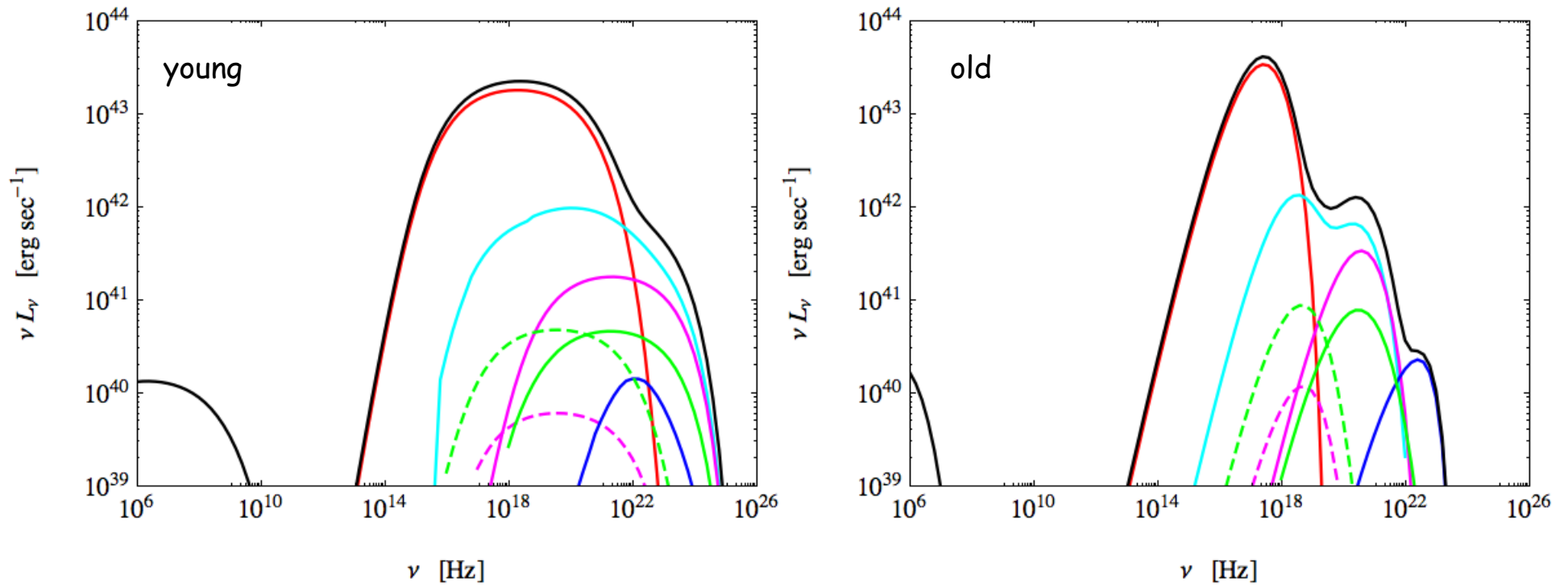


Table 6: Model C: young radio halo

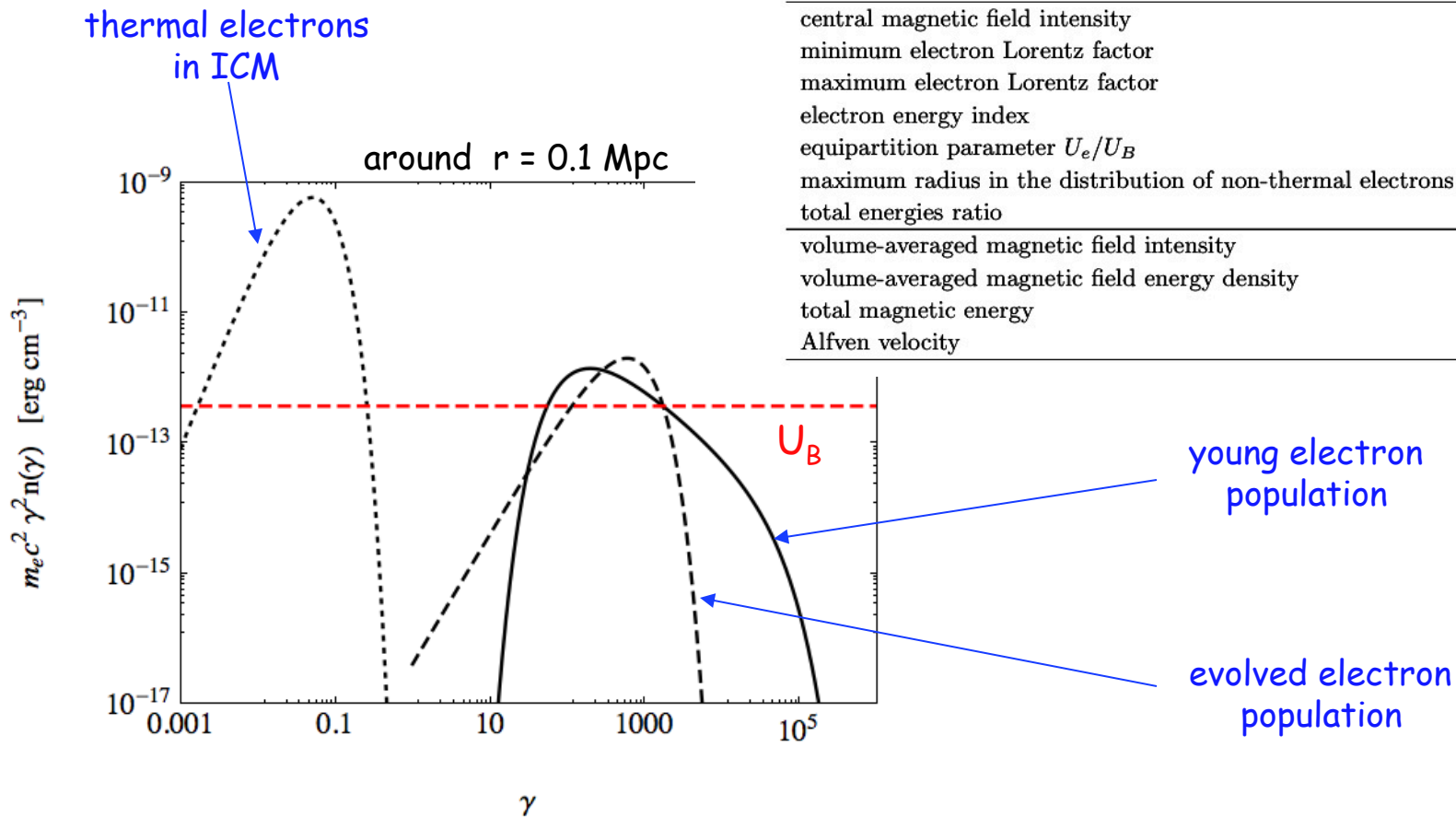
Quantity	Symbol	Model value
central magnetic field intensity	B_0	$3 \mu\text{G}$
minimum electron Lorentz factor	γ_{min}	200
maximum electron Lorentz factor	γ_{max}	3×10^4
electron energy index	s_e	3
equipartition parameter U_e/U_B	η_{eq}	10
maximum radius in the distribution of non-thermal electrons	$r_{\text{max},e}$	$0.1 r_{\text{vir}}$
total energies ratio	E_e/E_{th}	10^{-4}
volume-averaged magnetic field intensity	$\langle B \rangle$	$0.5 \mu\text{G}$
volume-averaged magnetic field energy density	$\langle U_B \rangle$	$10^{-14} \text{ erg cm}^{-3}$
total magnetic energy	E_B	$2 \times 10^{60} \text{ erg}$
Alfven velocity	v_A	$10^{-4} c$

MODEL C:

- High magnetization
- Electrons distributed within the cluster core

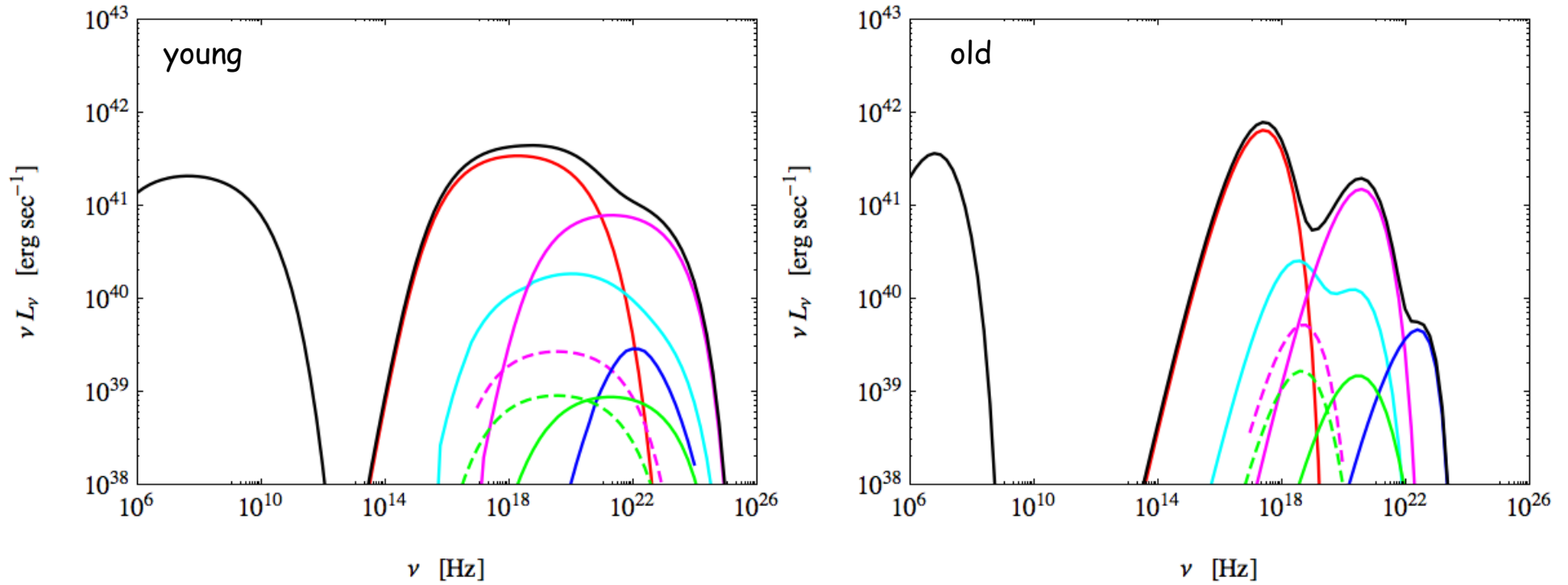
Table 7: Model C: old radio halo

Quantity	Symbol	Model value
central magnetic field intensity	B_0	$3 \mu\text{G}$
minimum electron Lorentz factor	γ_{min}	1
maximum electron Lorentz factor	γ_{max}	300
electron energy index	s_e	0
equipartition parameter U_e/U_B	η_{eq}	10
maximum radius in the distribution of non-thermal electrons	$r_{\text{max},e}$	$0.1 r_{\text{vir}}$
total energies ratio	E_e/E_{th}	10^{-4}
volume-averaged magnetic field intensity	$\langle B \rangle$	$0.5 \mu\text{G}$
volume-averaged magnetic field energy density	$\langle U_B \rangle$	$10^{-14} \text{ erg cm}^{-3}$
total magnetic energy	E_B	$2 \times 10^{60} \text{ erg}$
Alfven velocity	v_A	$10^{-4} c$



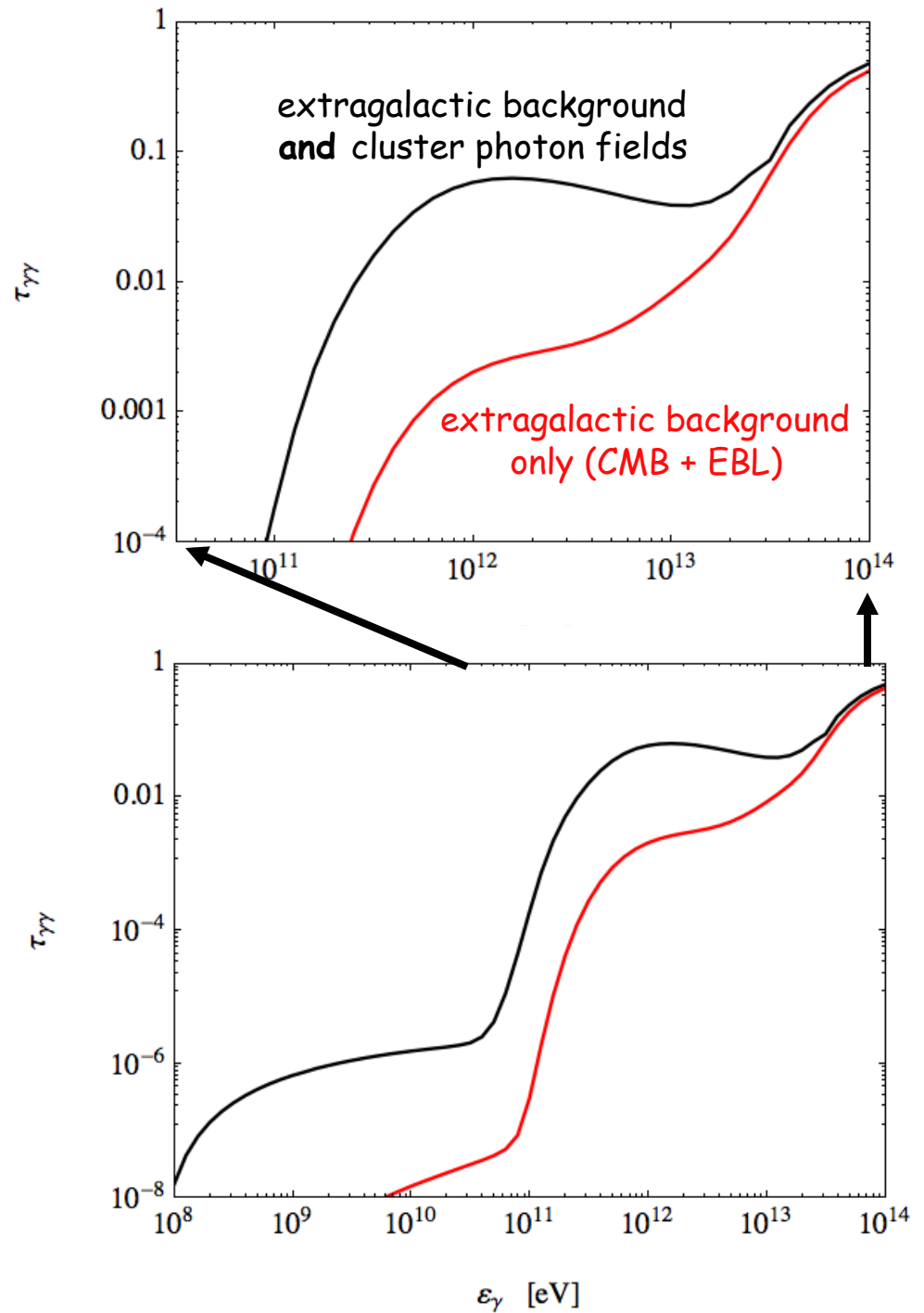
MODEL C:

- High magnetization
- Electrons distributed within the cluster core



Optical depth for gamma-ray photons emitted at the cluster center, propagating through the ICM, and annihilating on the soft photon fields provided by the cluster starlight, dust emission, and bremsstrahlung.

Note that for example M87 in the Virgo cluster as well as NGC 1275 in the Perseu cluster are established gamma-ray emitters (Fermi/LAT, IACTs)!



CONCLUSIONS

Cluster photon fields (including starlight, dust emission, and bremsstrahlung of a hot gas) may play an important role in shaping the high-energy non-thermal emission of intra-cluster medium.

- 1) Low magnetization of clusters hosting giant radio halos is excluded, since otherwise the inverse-Compton upscattering of background & cluster soft photon fields by radio-emitting electrons would violate the current upper limits in hard X-rays and in gamma-rays (roughly $L_\gamma < 10^{42}$ erg/s)
- 2) About 10% of 0.1-100 TeV photons emitted at the cluster center (by a central AGN) is expected to be absorbed within the inner parts of a cluster, due to the photon-photon annihilation on infrared-to-ultraviolet cluster photon fields; as a result, a substantial amount of very high-energy electrons may be injected into the ICM, depending on the gamma-ray duty-cycle of a central AGN
- 3) Presence of relic giant non-thermal halos in evolved clusters may be probed not only at the lowest accessible radio frequencies by instruments like LOFAR, but also at hard X-rays and in gamma-rays by modern and future instruments, due to inverse-Compton up-scattering of cluster photon fields by relic electrons
- 4) Because of the dependence of cluster photon fields on cluster-centric radius, the resulting high-energy emission of ultrarelativistic electrons present within the ICM depends crucially not only on the electron energy distribution (\rightarrow the age of a non-thermal halo), but also on a spatial distribution of non-thermal electrons (\rightarrow the origin of halo electrons)